Hybrid Approach to Retinal Tracking and Laser Aiming for Photocoagulation

Cameron H. G. Wright,[†] **R. Daniel Ferguson,**[‡] **H. Grady Rylander III,**[*]
Ashley J. Welch,[*] **and Steven F. Barrett**[†]

[†]U.S. Air Force Academy, Department of Electrical Engineering, USAF Academy, Colorado 80840;
[‡]Physical Sciences Inc., Andover, Massachusetts 01810; [*]University of Texas at Austin,
Biomedical Engineering Program, Austin, Texas 78712

Abstract

The initial experimental results of a new hybrid digital and analog design for retinal tracking and laser beam control are described. The results demonstrate tracking rates that exceed the equivalent of 60 deg per second in the eye, with automatic creation of lesion patterns and robust loss of lock detection. Robotically assisted laser surgery to treat conditions such as diabetic retinopathy and retinal tears can soon be realized under clinical conditions with requisite safety using standard video hardware and inexpensive optical components.
© 1997 Society of Photo-Optical Instrumentation Engineers. [S1083-3668(97)00602-3]

Keywords photocoagulation; retinal surgery; retinal tracking; ophthalmology.

1 Introduction

Retinal photocoagulation is the most widely used laser procedure employed today.[1] It is used to treat thousands of patients each year and is the recommended procedure for conditions such as diabetic retinopathy (requiring up to 3000 therapeutic lesions in each eye), retinal tears, and macular degeneration. Today, however, the procedure is performed manually and suffers from several drawbacks.[2] These include the fact that:

- It is time-consuming and often very tedious for both patient and ophthalmologist.
- The laser pointing accuracy and safety margin are limited by the ophthalmologist's manual dexterity and the patient's ability to hold his or her eye still.
- There can be complications from both over- and undertreatment.

For many years there has been a need to automate the process of placing lesions on a patient's retina at specific locations while protecting the critical vision anatomy.[3–5] However, one of the main obstacles to achieving this task has been the ability to track the retina and compensate for any movement with sufficient speed during photocoagulation.

This paper describes the initial results for a new hybrid digital/analog subsystem for retinal tracking and laser beam control that has been integrated into the development system known as CALOSOS: computer-aided laser optical system for ophthalmic surgery. CALOSOS will be able to create therapeutic retinal lesions of a specified number, location, and size in minimal time with little or no human intervention.

2 Tracking Requirements

Even when a patient is visually fixated on a motionless object, small eye motions occur continuously.[6] For the greatest safety and pointing accuracy, a retinal laser surgery system must compensate for an eye that is always moving. Even for lesion sites in the periphery, inadvertent eye movement could bring the fovea into the laser's path. CALOSOS will adjust the laser pointing system to keep the laser spot at the appropriate retinal location within a specified range of eye movements. For eye movements that exceed the tracking capability of CALOSOS, the system will close the laser shutter and initiate a relock sequence before reopening the shutter and continuing. The normally closed laser shutter can only open when an active signal is sent from the computer controller; this fail-safe design also protects against instances of patient blinking, power failure, or other system malfunction.

An extensive requirements definition phase was conducted for the design of CALOSOS,[7] and the primary conclusions are shown in Table 1. For this initial proof-of-concept design, only normal treatments for diabetic retinopathy and retinal tears were considered when arriving at these specifications. More position-critical treatments, such as for macular degeneration, would demand correspond-

Address all correspondence to Cameron H. G. Wright. E-mail: cwright@tesla.usafa.af.mil

Table 1 Summary of primary CALOSOS design specifications, suitable for treatment of diabetic retinopathy and retinal tears.

Function	Performance	
Retinal tracking	$\geqslant$10 deg/s	5-ms response time
Laser pointing	100 μm accuracy	5-ms response time
Lesion control	Uniform within 5%	5-ms response time

ingly more stringent specifications. Note that the requirements in Table 1 most germane to this article are the specified tracking capability of $\geqslant 10$ deg/s and the associated 5-ms response time. The 10 deg/s figure is the *minimum* capability for a usable system. Anything less would lose lock too often to be useful in a clinic; anything more (assuming no significant cost impact) would make the system more useful and attractive to the clinician. Note that if CALOSOS does lose lock, the laser is immediately turned off until lock can be reestablished—thus ensuring patient safety. While the eye is capable of moving at velocities in excess of 500 deg/s, conjugate eye fixation lowers this maximum to roughly 50 deg/s;[6] typical velocities with fixation are on the order of a few deg/s. Fixation also makes rotation of the eye negligible;[8] thus the retinal tracker need only detect and compensate for translation. The 5-ms response time specified in Table 1 is more difficult to achieve and is driven by the nominal clinical irradiation times of 100 ms. If a standard RS-170 camera (an important cost factor) is used to acquire the images, the 30 frame/s rate pushes the minimum possible response time to 33 ms. Previous attempts to design a system capable of tracking the retina, steering the laser, and automatically creating user-specified lesion patterns had a maximum tracking capability of 2 deg/s and a response time of more than 143 ms;[4,8] this is unacceptable for clinical use. Even at its present state of development, CALOSOS dramatically improves on this performance and exceeds the clinical tracking requirement of Table 1.

Note that, based upon inputs from practicing ophthalmologists, CALOSOS is designed to eliminate the need for a contact lens or for a retrobulbar injection. This is consistent with the goal for a system that provides the maximum comfort and safety for the patient.

3 TRACKING METHODS

Many methods have been devised for eye tracking, but most are designed to monitor the anterior eye and cornea. In order to place retinal lesions with acceptable accuracy, a system must track the retina directly and compensate for any movement.[9] A few methods of tracking the retina directly have been devised in recent years.[8–11] For CALOSOS, however, the choice of tracking methods is quite lim-

ited. When one accounts for the need to integrate (at the lowest reasonable cost) a photocoagulator laser control and pointing subsystem, an automatic lesion pattern generation subsystem, a lesion growth monitoring and control subsystem, and the retinal tracking subsystem of choice, with response times of 5 ms—and have it all work together seamlessly—then the most attractive tracking method is some variation of Barrett's digital technique,[8] which is briefly summarized below. This system is consistent with recommended algorithms for the rigid-body, translation-only tracking problem.[12]

3.1 DIGITAL TRACKING

CALOSOS is a computer-centric design. The computational requirements of the system, from laser pointing commands to automatic generation of lesion patterns, can be accomplished using an inexpensive microprocessor-based system such as a PC. A retinal image is obtained by using a CCD camera attached to the video port of a standard fundus camera and narrowband fundus illumination centered at 568 nm. A relatively high contrast image with a bright fundus and dark blood vessels is thus obtained.[13] A frame grabber then digitizes the image and places it in the main computer memory for processing. The fundus image features giving the best contrast and most suitable as tracking features are the major blood vessels. We employ a variable-width (often called *elastic* in the literature) one-dimensional template using only four pixels each, which has a maximum response when centered over a blood vessel. This is illustrated in Figure 1 for an ideal image and a single-width template. Note that the template response,

$$R = \frac{P1 - P2 - P3 + P4}{P1 + P2 + P3 + P4} \qquad (1)$$

is normalized and is therefore robust in the presence of image illumination variations and the less than ideal contrast of real-world fundus images. The image region between pixel P2 and P3 is the elastic region, which is adjusted according to the width of the blood vessel by seeking the greatest response R of Eq. (1). The width of the template is thus defined as the distance, in pixels, between P2 and P3 inclusive. The highest centered template response occurs for widths equal to the blood vessel width.

In order to track retinal images, we need a two-dimensional template. Six (three horizontal, three vertical) 1-D templates are combined into a 2-D tracking template by locking in the relative offsets of each 1-D template from a given template origin, where the 2-D template response is the sum of the 1-D template responses. Once defined, the 2-D template is scanned over the current image, and the point of maximum 2-D template response represents the updated location of the template origin. If
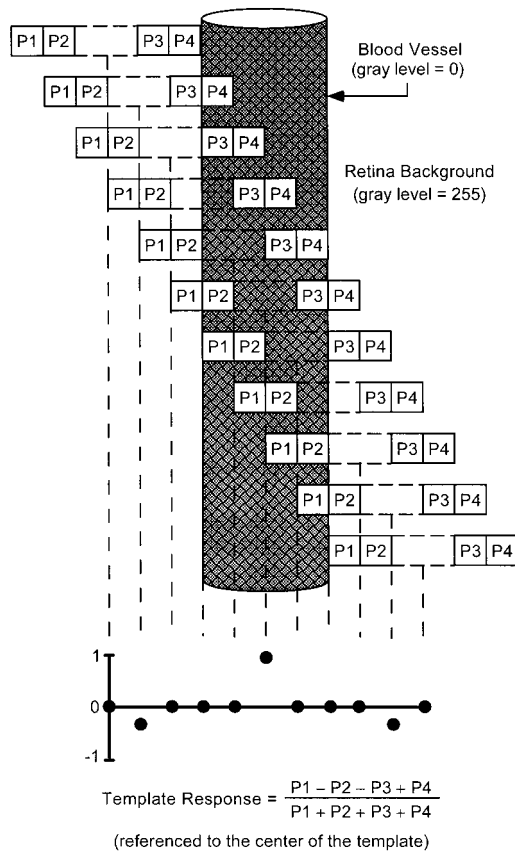
Fig. 1 Response of a 1-D template in the vicinity of a blood vessel.

Fig. 2 Conceptual view of the 2-D tracking template on a human fundus.

the maximum response is significantly different from the expected response, a loss of lock condition is detected. To select appropriate 1-D templates, the computer scans the reference image over some user-designated region, looking for the highest responding horizontal and vertical templates, with the first horizontal template defined as the 2-D template origin. By splitting the template selection search region into three equal areas and confining a horizontal/vertical template pair to each region, the software ensures that the selected templates are spatially distributed across the search region. This reduces the possibility of false positives.

A conceptualized view of the templates on an image of the fundus is shown in Figure 2. This 2-D template can be used to determine eye movement between video frames. The technique is highly efficient because it only needs to examine 24 pixel values for the entire 2-D template. Earlier work by Barrett found that proposals to use a coarse/fine search strategy for speed resulted in an unacceptable number of false positives.[8] Instead, we implement a "limited exhaustive search" routine using the 2-D template, achieving better than 99% correct registration (within a 100 μm error radius on the retina). The search is "limited" because the search area is restricted to pixels within the radius of anticipated maximum eye movement between frames;
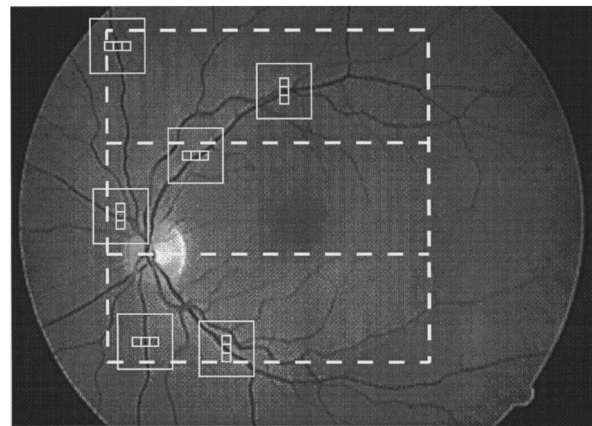
this maximizes the speed of the retinal tracking algorithm.

The required minimum search area is determined by the spatial dimensions of the image pixels, the maximum anticipated eye velocity, and the image frame rate. As an example, assume a square pixel spatial dimension of 32 μm per side on the retina (typical for a 640 × 480 RS-170 CCD camera using the specified CALOSOS optics), a maximum fixated eye velocity of 50 deg/s (explained in the previous section), and a frame rate of 30 frames/s (the speed of an RS-170 camera). Recall that 1 deg is equivalent to approximately 291.5 μm on the human retina at the posterior pole.[14] Then for this example the tracking algorithm must search in each direction S pixels defined as:

$$S = \frac{(50 \text{ deg/s})(291.5 \text{ } \mu\text{m/deg})}{(30 \text{ fps})(32 \text{ } \mu\text{m/pixel})} = 15.18 \approx 15 \text{ pixels.}$$

(2)

Since S is the distance the eye can travel in any direction, the search window would have to be at least $2S = 30$ pixels across. For a 2-D image, the rectangular search window is $2S \times 2S$, and thus the required computation time varies with $4S^2$. The faster the computer, the faster the eye velocity that can be tracked. For more detail about the basic digital tracking technique, see Ref. 8.

The digital tracking method described above has many advantages. For example, once the 2-D template has established its origin on the image, a Cartesian coordinate system is defined globally for the fundus image, which greatly facilitates the integration of lesion pattern creation and laser pointing. The digital method is also very flexible because of its software implementation. A key disadvantage of this method is its response time. For example, for lowest cost, a standard RS-170 camera should be used, but as previously stated, this 30 frame/s device forces the minimum possible response time to 33 ms (plus overhead). To meet the requirement of
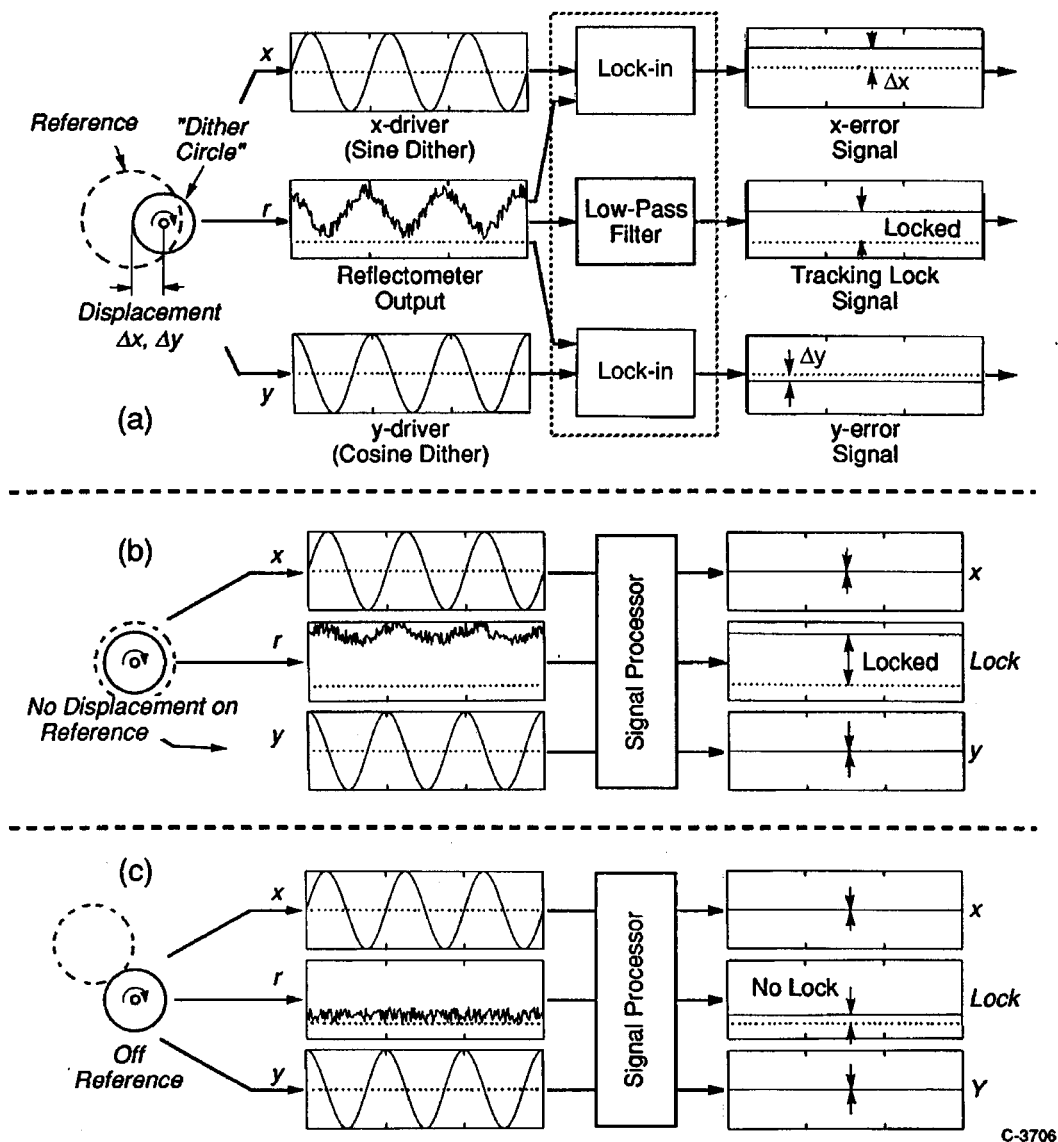
Fig. 3 Generation of analog tracking feedback signals from a confocal reflectometer.

a 5-ms response time, a camera with a frame rate of more than 200 frames/s would have to be used. Not only is this prohibitively expensive, but it cannot be used with standard monitors or VCRs, and the short integration time of light energy on the CCD array adversely affects fundus image quality. Hence we sought some other alternative.

3.2 ANALOG TRACKING

To overcome the frame rate problems of our digital tracking method, we investigated a novel analog tracking technique.

3.2.1 Generating Analog Tracking Signals

Recall that a laser-induced retinal lesion is more highly reflective than normal retinal tissue: it looks bright compared with the darker surrounding tissue in fundus images. We use that feature to our advantage by moving a low-power[15] secondary laser beam in a small circle around a designated reference lesion, and detecting the returning light with a confocal reflectometer.[16,17] At any given instant when this "dithered" beam is pointed on the reference lesion, the reflectometer signal is high; when it is pointed off the lesion the reflectometer signal is low. Thus the reflectometer output signal varies synchronously (when corrected for phase shifts) with the periodic dither signal that drives the dithering mirrors, as shown in Figure 3 and discussed more completely in the following paragraphs.

The dither beam confocal reflectometer output is processed to yield Δx and Δy error signals, which initially increase as the dithered tracking beam moves farther from the center of the reference lesion. The error signals contain all the information needed to redirect the tracking beam back to the

center of the reference lesion, thereby minimizing the error signal. By integrating these error signals over time, so that cumulative errors produce net displacement voltages that are coupled to the main steering mirrors in the tracking beam path, arbitrary motions of the reference lesion relative to the tracking beam can be followed. Since the reference lesion is fixed with respect to the retina, this results in retinal tracking. Such a control system is a variation on the familiar servo loop concept.

Figures 3(a) to 3(c) depict some representative dither circle signals and the resulting reflectometer signals. Phase-sensitive detection is accomplished with lock-in amplifiers,[18] which are simply analog multipliers (mixers) followed by low-pass filters, which produce dc offset voltages proportional to the amplitude component of the reflectometer signal which is in phase with the associated X or Y dither signal. The resulting pair of error voltages constitutes a tracking correction vector that is relayed to the main steering mirrors. Note that in addition to the Δx and Δy error signals provided by the two lock-in amplifiers, a third signal is extracted from the reflectometer output: the average value of the returning light from the dither beam. Figure 3(a) shows a case in which the dither circle is displaced along the x axis (but not the y axis) relative to the reference lesion. There is a Δx error signal proportional to the displacement, and a zero Δy error signal. Note that the average value, or dc level, of the confocal reflectometer is significantly greater than 0. Figure 3(b) represents a case in which the dither circle is centered and locked on the reference lesion (the eye may or may not be stationary at this instant) so that null error signals are produced. Again the dc level of the confocal reflectometer is significantly greater than 0. In Figure 3(c), the dither circle has ''fallen off'' the reference lesion completely and the error signals are meaningless. However, note that the dc level of the confocal reflectometer signal is now very low. This low dc value condition results in a loss of lock condition being detected.

3.2.2 Analog Tracking Performance Metrics

The maximum tracking speed on the retina is related to the dither frequency and reference lesion size. The basic relationship is

$$v_{\max} = k D f_d,\qquad(3)$$

where $v_{\max}$ is the maximum eye velocity that can be tracked, k is a system-dependent dimensionless constant related to the error signal gain (which affects its detectability) and the transient response of the associated circuitry (which determines how quickly the error signal can change values), D is the diameter of the relatively circular reference lesion, and f_d is the oscillation frequency of the dither beam. For example, at a retinal velocity of 50 deg/s, the retina moves at $\simeq 14.6$ mm/s. With a 2-kHz

dither frequency, this corresponds to a retinal displacement of approximately 7.3 μm per dither cycle. If we assume a reference lesion diameter of 400 μm, and a tracking beam initially centered on the reference lesion, then over 54 dither cycles would occur before the tracking beam ''fell off'' the reference lesion by a distance of D, assuming no tracking correction. This relatively large number of cycles per reference lesion diameter affords sufficient opportunity to integrate the signal, generating a detectable tracking signal that can correct for the motion before tracking lock is lost. The value of k can be determined empirically by adjusting the integration time for the tracking error signal until the system operates satisfactorily. This integration time equals some number of cycles of the dither frequency, and the inverse of the number of cycles equals k. For the analog electronics used for CALOSOS, the value of k was determined in this way to be approximately 0.1, yielding a theoretical maximum retinal tracking velocity of over 274 deg/s with a 400 μm reference lesion—if everything works perfectly. As will be described in the results section, the real-world achievable tracking velocity is much less.

The response time τ of the analog tracking system is inversely proportional to k from Eq. (3), since k is a measure of how many dither cycles are needed to generate a detectable error signal, which is related to how quickly the error signal can change values. Thus τ can be determined using the relationship

$$\tau = \frac{1}{k \cdot f_d}.\qquad(4)$$

Increasing the dither frequency f_d would make the system faster, but since the galvanometers driving the dither mirrors are operating in superresonant mode, further increases in frequency would be difficult with the inexpensive galvanometers used for the prototype. Taking the inverse of the empirically determined k for CALOSOS yields 10 cycles of the 2-kHz dither signal, which equals a response time of $\tau = 5$ ms.

The theoretical accuracy of the analog tracking system is a complex relationship of several factors. It is proportional to the overall detectability of the reflected tracking beam, the ratio of the tracking beam spot diameter to the reference lesion diameter, the ratio of the dither circle diameter to the reference lesion diameter, the tracking beam cross-sectional profile, and perhaps other factors. Quantitative analysis of this figure of merit is still being investigated, but the bounding value of tracking accuracy can be determined from the retinal velocity and the tracking system response time. For the specified accuracy requirement of 100 μm, and the analog tracking response time of 5 ms determined above, the retinal velocity must be such that the eye moves less than or equal to 100 μm in 5 ms. This

yields a maximum retinal velocity of 20 mm/s, which is equivalent to 68.6 deg/s eye velocity.

3.3.3 Analog Tracking Implementation

The analog tracking system creates the dither signal in a simple, symmetrical fashion. By driving the *x* and *y* dithering mirrors 90 deg out of phase at identical amplitudes, a ''dither circle'' is produced. The mirrors are attached to a pair of orthogonally mounted galvanometers and driven at 2 kHz. This driving frequency is well above the loaded resonance frequency for these scanners ($\simeq 500$ Hz), but because only small amplitudes were required for the dithering motion, this superresonant driving did not present a problem. The first dither mirror is a typical first-surface mirror. The second dither mirror is actually a beamsplitter instead of a mirror. In reflection, it serves as the second dither axis ''mirror.'' In transmission, however, it serves as a nondeflecting window through which the high-power coagulating beam passes on the way to the main steering mirrors (see Figure 4). This design innovation minimizes (and equalizes) the optical path lengths between the optical surfaces in both the tracking and coagulating beam legs of the optical system, reduces the number of required components, and allows all four steering mirrors to ''share'' the conjugate plane of the retina as required for coupling into the eye (see Figure 5). The confocal reflectometers were custom fabricated and were designed to be mounted directly in standard optical mounts.

The main steering mirrors are farther down the optical train than the dither mirrors. In order to be certain to accommodate the range of angular motions of the dither mirrors, much larger mirrors were selected for the main steering galvanometers. The design ramification of this is that the main steering galvanometers for analog tracking need to drive larger inertial loads than they do in the digital tracking implementation. Note that an engineering analysis of the galvanometers and the associated laser pointing subsystem, while a contributor to the final accuracy of CALOSOS, is beyond the scope of this paper.

The analog tracking technique relies upon an optimized optical design to couple light into and out of the patient's eye. The overall layout is shown in Figure 4. More detail of the light path coupling into and out of the eye is shown in Figure 5. Note the critical alignment of both the retinal conjugate plane and the pupillary conjugate plane shown in Figure 5 to ensure proper laser delivery and reflectometer performance.

The signal processing and control circuitry for the analog tracking technique is implemented in hardware using inexpensive components. It can track and stay locked at very high retinal velocities. The limiting factor is not the circuitry, but the resonance frequency of the galvanometers used to drive the beam steering mirrors. In our first prototype, we found that the equivalent of better than 60 deg/s at the retina was achievable. With smaller, lighter galvanometers, we expect to more than double that performance.

While extremely fast compared with the digital tracking method, the analog tracker has some significant disadvantages for use with CALOSOS. If used alone, no coordinate system data is provided by the analog tracker, making the integration of lesion pattern creation and laser pointing subsystems much more difficult. Even more important, the analog tracker is a purely local device—once the dither beam has fallen off the reference lesion and lost lock, the system has no idea where the tracking beam is pointing relative to the reference lesion and no way to relock the tracking beam. With this in mind, we decided to combine the digital and analog techniques into a single hybrid implementation.

4 TRACKING RESULTS: HYBRID SYSTEM

To test the tracking results of the hybrid implementation, we placed an albumen eye phantom on the pen armature of an *XY* plotter, located at the retinal conjugate plane (see Figure 6). The eye phantom consisted of fresh clear egg white at 22 °C contained in a petri dish with a highly absorbing layer of Kapton® film* on the bottom. The raw egg white exhibits optical properties close to the neural retina, and the Kapton absorbs laser energy (at the argon laser wavelengths) in place of the retinal pigment epithelium. When the laser irradiates the phantom, light passes through the egg white and is absorbed by the Kapton. This causes significant heat generation, which in turn will locally coagulate the egg white. As the egg white coagulates, the scattering coefficient increases and a white ''lesion'' appears.

Testing with the phantom at the retinal conjugate plane is optically equivalent to irradiating the actual retina, yet simplifies the experimental setup. With the *XY* plotter moving the eye phantom at various speeds and patterns, we used the prototype to create both individual lesions and rectangular patterns of lesions. As long as the tracking subsystem remained locked, we were able to produce accurate, motion-stabilized lesions on the eye phantom at will. The repeatable maximum tracking velocities we achieved are shown in Table 2, and represent an improvement of more than thirty times the maximum tracking velocity of previous designs. The retinal equivalent velocity is calculated assuming a 3:1 optical demagnification from the retinal conjugate plane to the retina, and assuming 291.5 μm/deg on the retina.[14] For example, a velocity on the *XY* plotter of 6 cm/s at the retinal conjugate plane would equate to 2 cm/s on the retina near the posterior pole, which would equate to an angular

---

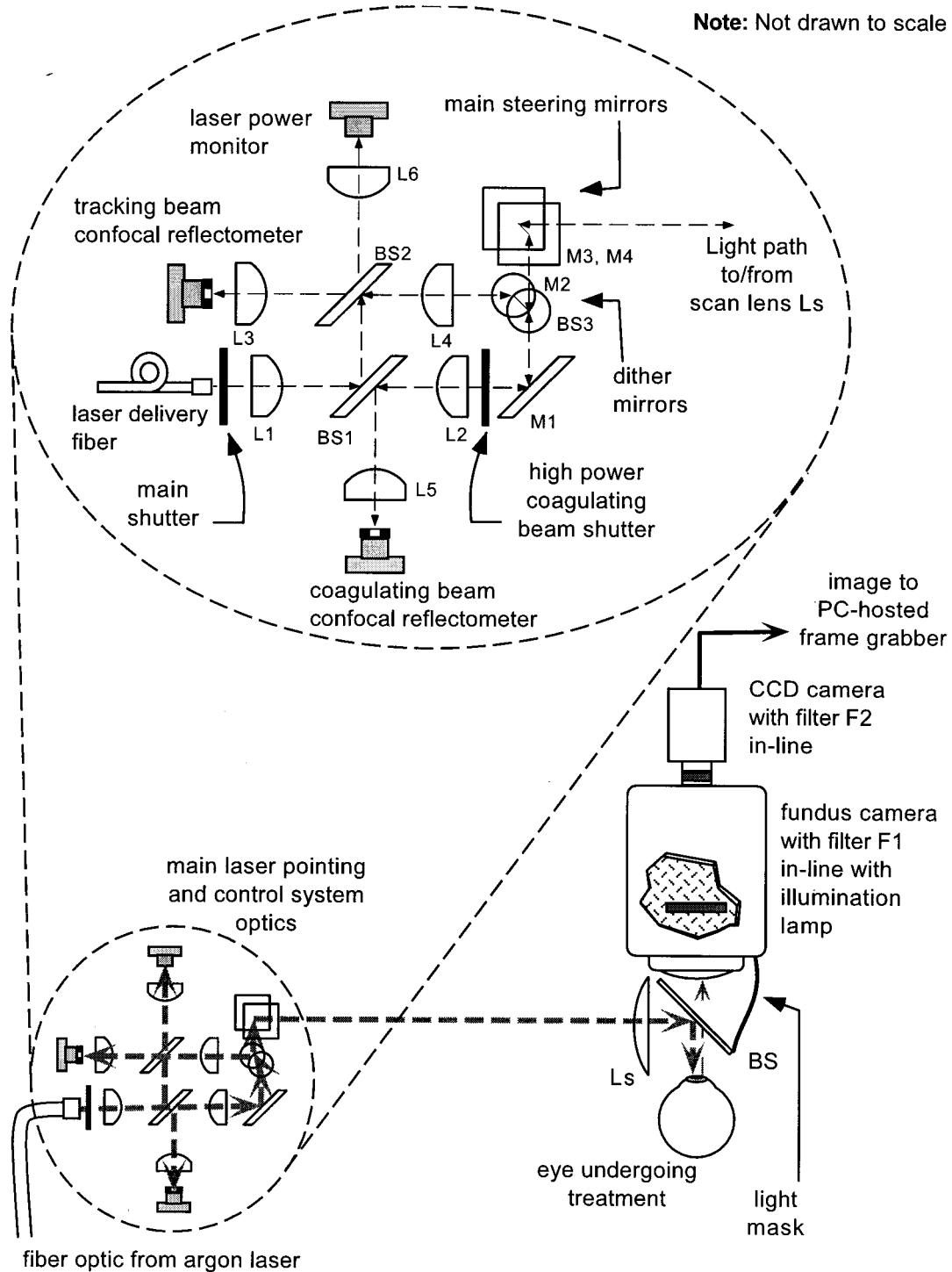*Constructed of polyimide, Kapton is a registered trademark of the 3M Corporation.

Fig. 4 Optical schematic for the analog tracking technique. An expanded view is inset to show needed detail. The tracking beam reflectometer detects the dither signal and the coagulating beam reflectometer is used to control therapeutic lesion formation. Main beam steering mirrors: M3 and M4. Dithering performed by M2 and BS3.

velocity of 68.6 deg/s. The response time of the analog tracker meets the 5 ms requirement, as shown in the evaluation of Eq. (4) above.

While the analog subsystem tracked the movements of the eye phantom and compensated the

main beam steering galvanometers to negate that movement, the digital subsystem used the image coordinate system (defined by the 2-D template) to automatically create user-specified lesion patterns with no operator intervention. We created several
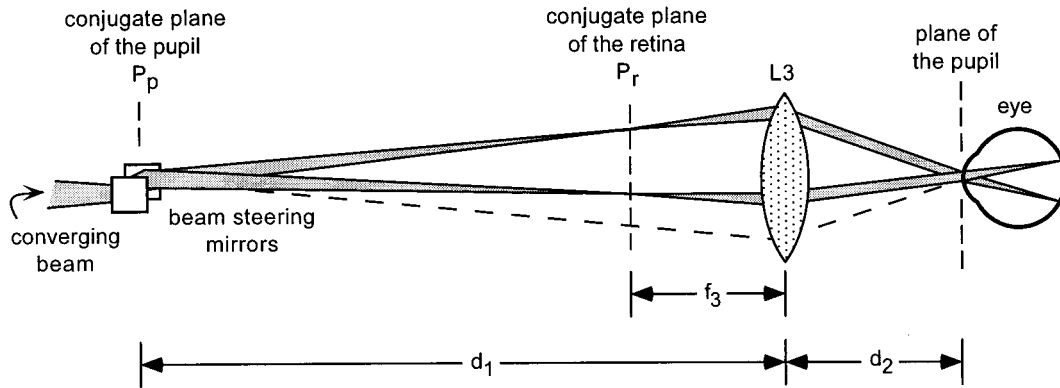
Fig. 5 The light path of the analog tracking setup shows how incident and reflected light of the tracking and coagulating beams is coupled into and out of the eye. Not drawn to scale.

rectangular 3×4 patterns of lesions that showed no observable distortion despite the rapid movementof the eye phantom on the XY plotter. The positional accuracy of the individual lesion sites was better than 0.5 mm (the limit of our measuring device) at the retinal conjugate plane, which is equivalent to better than 166 μm accuracy on the retina. Further tests will more closely measure the positional accuracy, which we expect will meet the 100-μm requirement. Note that this positional accuracy is dependent upon the laser pointing subsystem, which (as stated earlier) is not addressed in this paper.

5 SUMMARY AND CONCLUSIONS

This paper concentrated on improvements to the design approach for tracking the moving retina, with emphasis on tracking speed and system response time. We found that when digital and analog tracking systems are combined, their individual strengths are highly complementary. The speed problems of the digital technique are compensated for by the fast analog tracking capability; the lack of information on global fundus position inherent in the analog technique is compensated for by the Cartesian coordinate system defined by the digital tracker's 2-D template. Thus the tracking speed and response time requirements for CALOSOS can be met using inexpensive off-the-shelf components. Future improvements will increase tracking speed, positional accuracy of the lesion patterns (which is nearing the requirement for most photocoagulation procedures), and the level of analog/digital integration.

The hybrid technique described here, when combined with other subsystems of CALOSOS, will soon make it possible to use robotically assisted laser surgery to treat ophthalmic conditions such as diabetic retinopathy and retinal tears under clinical conditions with the requisite safety margin.
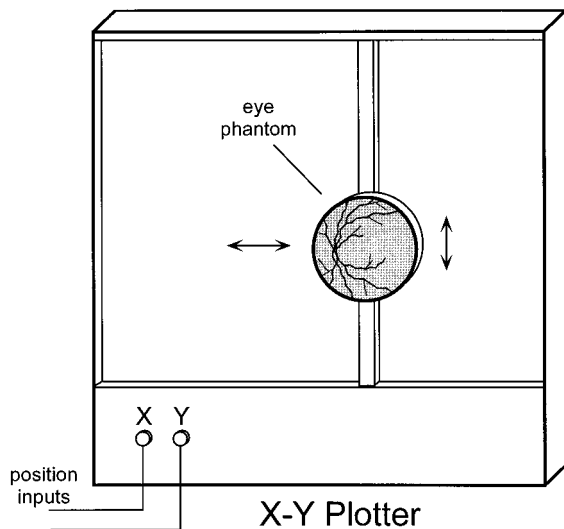

Fig. 6 Illustration of an eye phantom attached to the pen holder armature of an XY plotter to produce simulated eye movements.

Table 2 Results of the hybrid tracking subsystem with an eye phantom located on an XY plotter at the conjugate retinal plane.

Waveform	Tracking limit	Retinal equivalent
Sine	1 Hz, 2 cm p-p, 6 cm/s	68.6 deg/s
Sine	9 Hz, 2 mm p-p, 6 cm/s	68.6 deg/s
Triangle	1 Hz, 2.5 cm p-p, 5 cm/s	57.2 deg/s
Triangle	9 Hz, 2 mm p-p, 6 cm/s	68.6 deg/s

Note: 9 Hz was the maximum XY plotter response. Retinal demagnification of 3:1 assumed.

Acknowledgments

REFERENCES

1. J. M. Krauss and C. A. Puliafito, ''Lasers in ophthalmology,'' *Lasers Surg. Med.* **17**(2), 102–159 (1995).
2. G. L. Spaeth, Ed., *Ophthalmic Surgery: Principles and Practice*, W. B. Saunders, Philadelphia, PA (1982).
3. R. Birngruber, V. P. Gabel, and F. Hillenkamp, ''Fundus reflectometry: A step towards optimization of retina photocoagulation,'' *Mod. Prob. Ophthalmol.* **18**, 383–390 (1977).
4. M. S. Markow, A. J. Welch, H. G. Rylander III, and W. S. Weinberg, ''An automated laser system for eye surgery,'' *IEEE Eng. Med. Biol.* **8**(4), 24–29 (1989).
5. S. F. Barrett, C. H. G. Wright, M. R. Jerath, R. S. Lewis II, B. C. Dillard, H. G. Rylander III, and A. J. Welch, ''Computer-aided retinal photocoagulation system,'' *J. Biomed. Opt.* **1**, 83–91 (1996).
6. W. Kosnik, J. Fikre, and R. Sekuler, ''Visual fixation stability in older adults,'' *Invest. Ophthalmol. Vis. Sci.* **27**, 1720–1725 (1986).
7. S. F. Barrett, C. H. G. Wright, E. D. Oberg, B. A. Rockwell, C. P. Cain, M. R. Jerath, H. G. Rylander III, and A. J. Welch, ''Integrated computer-aided retinal photocoagulation system,'' in *Proc. SPIE* **2673** (1996).
8. S. F. Barrett, M. R. Jerath, H. G. Rylander III, and A. J. Welch, ''Digital tracking and control of retinal images,'' *Opt. Eng.* **33**, 150–159 (1994).
9. D. P. Wornson, G. W. Hughes, and R. H. Webb, ''Fundus tracking with the scanning laser ophthalmoscope,'' *Appl. Opt.* **26**, 1500–1504 (1987).
10. T. Bantel, D. Ott, and M. Rueff, ''Global tracking of the ocular fundus pattern imaged by scanning laser ophthalmoscopy,'' *Int. J. Biomed. Comput.* **27**, 59–69 (1990).
11. M. S. Markow, H. G. Rylander III, and A. J. Welch, ''Real-time algorithm for retinal tracking,'' *IEEE Trans. Biomed. Eng.* **40**, 1269–1281 (1993).
12. L. G. Brown, ''A survey of image registration techniques,'' *ACM Comput. Surv.* **24**, 325–376 (1992).
13. F. C. Delori, E. S. Gragoudas, R. Francisco, and R. C. Pruett, ''Monochromatic ophthalmoscopy and fundus photography,'' *Arch. Ophthalmol.* **95**, 861–868 (1977).
14. D. G. Vaughan, T. Asbury, and P. Riordan-Eva, *General Ophthalmology*. Appleton & Lange, Norwalk (Connecticut), 13th ed., 1992.
15. American National Standards Institute, American National Standard for Safe Use of Lasers, ANSI Z136.1-1993.
16. J. H. Inderfurth, R. D. Ferguson, M. B. Frish, and R. Birngruber, ''Dynamic reflectometer for control of laser photocoagulation on the retina,'' *Lasers Surg. Med.* **15**, 54–61 (1994).
17. J. B. Pawley, Ed., *Handbook of Biological Confocal Microscopy*, 2nd ed., Plenum Press, New York (1995).
18. M. L. Meade, *Lock-In Amplifiers: Principles and Applications*. Peregrinus Ltd., London (1983).